



ELSEVIER

Contents lists available at ScienceDirect

Planetary and Space Science

journal homepage: www.elsevier.com/locate/pss

Grid-based mapping: A method for rapidly determining the spatial distributions of small features over very large areas

Jason D. Ramsdale^{a,*}, Matthew R. Balme^{a,b}, Susan J. Conway^{a,c}, Colman Gallagher^{d,e},
Stephan A. van Gasselt^f, Ernst Hauber^g, Csilla Orgel^{f,g}, Antoine Séjourné^h, James A. Skinnerⁱ,
Francois Costard^h, Andreas Johnssonⁱ, Anna Losiak^{k,l}, Dennis Reiss^m, Zuzanna M. Swiradⁿ,
Akos Kereszturi^o, Isaac B. Smith^p, Thomas Platz^{b,q}

^a Department of Physical Sciences, The Open University, Walton Hall, Milton Keynes, Buckinghamshire MK7 6AA, UK

^b Planetary Science Institute, Suite 106, 1700 East Fort Lowell, Tucson, AZ, USA

^c Laboratoire de Planétologie et Géodynamique – UMR CNRS 6112, 2 rue de la Houssinière – BP 92208, Nantes, 44322 Cedex 3, France

^d UCD School of Geography, University College, Belfield, Dublin 4, Ireland

^e UCD Earth Institute, University College, Belfield, Dublin 4, Ireland

^f Freie Universität Berlin, Institute of Geological Sciences, Planetary Sciences and Remote Sensing, D-12249 Berlin, Germany

^g DLR-Institut für Planetenforschung, Rutherfordstrasse 2, D-12489 Berlin, Adlershof, Germany

^h GEOPS-Geosciences Paris Sud, CNRS, Université Paris-Saclay, Université Paris Sud, Bat. 509, F-91405 Orsay, France

ⁱ US Geological Survey, Flagstaff, AZ 86001, USA

^j Department of Earth Sciences, University of Gothenburg, Box 460, SE-405 30 Gothenburg, Sweden

^k Institute of Geological Sciences, Polish Academy of Sciences, Podwale 75, 50-449 Wrocław, Poland

^l Department of Lithospheric Research, University of Vienna, Althanstrasse 14, A-1090 Vienna, Austria

^m Institut für Planetologie, Westfälische Wilhelms-Universität, Wilhelm-Klemm-Str. 10, 48149 Münster, Germany

ⁿ Department of Geography, Durham University, Durham DH1 3LE, UK

^o Research Centre for Astronomy and Earth Sciences, Csatka u. 6-8., 9400 Sopron, Hungary

^p Institute for Geophysics, University of Texas, J.J. Pickle Research Campus, Bldg. 196, 10100 Burnet Rd. (R2200), Austin, TX 78758-4445, USA

^q Max Planck Institut für Sonnensystemforschung, Justus-von-Liebig-Weg 3, 37077 Göttingen, Germany

A B S T R A C T

The increased volume, spatial resolution, and areal coverage of high-resolution images of Mars over the past 15 years have led to an increased quantity and variety of small-scale landform identifications. Though many such landforms are too small to represent individually on regional-scale maps, determining their presence or absence across large areas helps form the observational basis for developing hypotheses on the geological nature and environmental history of a study area. The combination of improved spatial resolution and near-continuous coverage significantly increases the time required to analyse the data. This becomes problematic when attempting regional or global-scale studies of metre and decametre-scale landforms. Here, we describe an approach for mapping small features (from decimetre to kilometre scale) across large areas, formulated for a project to study the northern plains of Mars, and provide context on how this method was developed and how it can be implemented.

Rather than “mapping” with points and polygons, grid-based mapping uses a “tick box” approach to efficiently record the locations of specific landforms (we use an example suite of glacial landforms; including viscous flow features, the latitude dependant mantle and polygonised ground). A grid of squares (e.g. 20 km by 20 km) is created over the mapping area. Then the basemap data are systematically examined, grid-square by grid-square at full resolution, in order to identify the landforms while recording the presence or absence of selected landforms in each grid-square to determine spatial distributions. The result is a series of grids recording the distribution of all the mapped landforms across the study area. In some ways, these are equivalent to raster images, as they show a continuous distribution-field of the various landforms across a defined (rectangular, in most cases) area. When overlain on context maps, these form a coarse, digital landform map.

We find that grid-based mapping provides an efficient solution to the problems of mapping small landforms over large areas, by providing a consistent and standardised approach to spatial data collection. The simplicity of the grid-based mapping approach makes it extremely scalable and workable for group efforts, requiring minimal

* Corresponding author.

E-mail address: jason.ramsdale@open.ac.uk (J.D. Ramsdale).

<http://dx.doi.org/10.1016/j.pss.2017.04.002>

Received 6 February 2017; Received in revised form 27 March 2017; Accepted 6 April 2017

0032-0633/ © 2017 Published by Elsevier Ltd.

user experience and producing consistent and repeatable results. The discrete nature of the datasets, simplicity of approach, and divisibility of tasks, open up the possibility for citizen science in which crowdsourcing large grid-based mapping areas could be applied.

1. Introduction

With increasing coverage of high-resolution images of the surface of Mars (e.g. Context Imager – CTX, ~6 m/pixel, [Malin et al., 2007](#), covering ~90% of the surface) we are able to identify increasing numbers and diversity of small-scale landforms. Many such landforms are too small to represent individually on regional maps, yet determining their presence or absence across large areas can form the observational basis for developing hypotheses on the geological nature and environmental history of a study area. The combination of improved spatial resolution with near-continuous coverage in spatial data means that sub-sampling of study areas is no longer needed when identifying landforms, but significantly more time is required to analyse the data. This becomes problematic when attempting regional or global-scale studies of metre and decametre-scale landforms. Here, we describe an approach for mapping small features across large areas formulated for a project to study the northern plains of Mars and provide context on how this method was developed and how it can be implemented.

The ISSI (International Space Science Institute) project that this study was a part of aimed to detail the geological and stratigraphic character of the martian northern plains, with particular regard to the role that near-surface ice has played in their morphological evolution through the mapping of surface ice-related features. It is thought ([Kreslavsky and Head, 2002](#); [Lucchitta et al., 1986](#); [Tanaka et al., 2005](#)) that the uppermost layers of the northern plains are largely sediments that have been shaped by processes involving water-ice, but no consensus has emerged on the origin and emplacement mechanism of the ice. [Kargel et al. \(1995\)](#) discuss several proposed mechanisms of emplacement including freezing of fluvial, lacustrine or marine wet sediments, air-fall deposition/condensation, shallow groundwater processes, or a combination of these different processes. Furthermore, although the spatial distributions of some landform types have been measured and correlated with latitude-controlled climatic processes (e.g. transverse aeolian ridges, TARs [Balme et al., 2008](#); [Berman et al., 2011](#); [Wilson and Zimbelman, 2004](#), viscous-flow features, VFFs; [Milliken et al., 2003](#), glacier-like forms, GLFs; [Souness et al., 2012](#), dunes; e.g. [Hayward et al., 2007](#)), broad-scale heterogeneity in surface features exists within latitude bands (e.g. Geology; [Tanaka et al., 2005](#), craters; [Barlow and Bradley, 1990](#); [Robbins and Hynes, 2012](#), latitude-dependant mantle, LDM; [Kreslavsky and Head, 2002](#)). This suggests that regional geology and climate have played a dominant role in the evolution of the northern plains, which requires a more detailed understanding of the relationships between the geological units of the northern plains, the boundary conditions, and the resulting geomorphic landforms.

Systematic, targeted geomorphological mapping of the spatial distribution of landforms thought to be indicative of ice in the regolith must be completed if we are to understand the geological evolution, environmental change and astrobiological potential (particularly whether sufficient liquid water was ever generated from ground-ice thaw; e.g., [Ulrich et al., 2012](#)) of the martian northern plains. The ISSI project aimed to answer the following science questions: (1) What is the distribution of ice-related landforms in the northern plains and can it be related to distinct latitude bands, different geological units, physiographic provinces, and/or topography? (2) What is the relationship between the LDM and (a) landforms indicative of ground ice and (b) other geological units in the northern plains?, (3) What are the distributions and associations of recent landforms indicative of thaw of ice or snow? This paper deals with the method used to answer these questions. We aim to submit companion science papers for Arcadia

Planitia, Utopia Planitia and Acidalia Planitia alongside a new study of northern plains impact crater morphology followed by a synthesis of findings and previous works.

Previous work on the Martian northern plains includes the first global geologic map of Mars, which was produced at a 1:25,000,000 scale on a photomosaic of 1–3 km/pixel Mariner 9 visible wavelength images ([Scott and Carr, 1978](#)). Viking images with spatial resolutions of up to 100 m/pixel were analysed, leading to the production of three 1:15,000,000 scale maps ([Greeley and Guest, 1987](#); [Scott and Tanaka, 1986](#); [Tanaka and Scott, 1987](#)). These maps were combined and digitised for surface age reconstruction ([Tanaka et al., 1988](#)) and later updated to a GIS format ([Skinner et al., 2006](#)). Later, MOLA (Mars Orbiter Laser Altimeter; [Smith et al., 1993](#)) global topographic elevation data with 463 m/pixel spatial resolution or better and 1 m vertical precision ([Smith et al., 1993](#)), THEMIS (Thermal Emission Imaging System) near-infrared (IR) day and night-time images at 100 m/pixel ([Christensen et al., 2004](#)) and CTX images provided an excellent base for the next generation, 1:15,000,000 scale northern hemisphere map ([Tanaka et al., 2005](#)). A new global geological map at 1:20,000,000 scale with up to date chronostratigraphy and resurfacing ages has recently been published ([Tanaka et al., 2014](#)).

The early Mariner 9- and Viking-based geological maps were drafted by hand onto image mosaics or air brushed onto manually produced shaded relief bases ([Batson et al., 1979](#)). With the development of geographic information system (GIS) software, planetary mapping has become increasingly digital with older maps being scanned and digitised to allow for direct comparisons with the modern maps and bases that are developed almost entirely within GIS software ([Tanaka et al., 2014](#)). Both the early and modern geological maps focus on boundary and unit mapping, recording the distribution of units and landforms on the planet's surface and placing them within a chronological framework.

Where geological maps focus on placing observations into stratigraphic units, geomorphological maps can be considered graphical inventories of landscape that catalogue landforms, surface, and subsurface materials ([Otto and Smith, 2013](#)). Geomorphological maps can be categorised as either basic/analytical or derived/specialized. While basic maps are more generic and display the observed features of a landscape, derived or thematic maps are topically focused for a specific study or application. Traditionally, the basis for constructing a geomorphological map has been the drawing of points, lines, and polygons to represent landforms and surface types onto a topographic and/or image base map. For example, the northern plains of Mars are generally divided into allostratigraphic (unconformity-bounded) units based upon their inferred primary (emplacement) physical features, areal extent, relative ages, and geologic associations ([Tanaka et al., 2005](#)). However, small-scale (large area) geological and geomorphological maps are only capable of representing the largest features and the regional basement materials, and cannot consistently include decametre-scale landforms or thin surficial covers of materials. Previous martian geomorphological studies of small features have generally incorporated a survey-style approach and identified single landforms (e.g. TARs; ([Balme et al., 2008](#); [Berman et al., 2011](#); [Wilson and Zimbelman, 2004](#)), VFFs; [Milliken et al. \(2003\)](#), GLFs; [Souness et al. \(2012\)](#), dunes; e.g. [Hayward et al. \(2007\)](#), craters; [Barlow and Bradley \(1990\)](#); [Robbins and Hynes \(2012\)](#), latitude-dependant mantle, LDM; [Kreslavsky and Head \(2002\)](#)). In most cases, these studies have used high resolution images that do not have a continuous spatial extent over the study area but instead are only small ‘windows’ sampling a subset of the true population of the features.

Where basic geomorphological mapping has been conducted on Mars, it has tended to be, at best, regional in scale (e.g. Valles Marineris; [Peulvast et al., 2001](#), Hellas Basin; [Kargel and Strom, 1992](#), Hale Crater; [Jones et al., 2011](#)) often including morphometrics and there has been no global basic geomorphological mapping effort aimed at the sub-kilometre scale landforms. This is largely due to the question of scale. The majority of identifiable ice-related landforms and terrain types are of metre to decametre scale and mapping them requires observations at 1:10,000 scale. This makes cataloguing their global spatial occurrence on a traditional 1:15,000,000 scale geomorphological global map an enormous task, first requiring the identification and classification of all visible, thematically relevant landforms in 1500 separate 1:10,000 mapping areas. However, a compromise between basic and derived thematic geomorphological mapping can be found in the grid-based mapping approach described in this manuscript. While not a replacement for geological or geomorphological mapping, grid-based mapping is a powerful approach that allows for systematic identification of the distribution of multiple landform types across very large continuous areas. We find that this approach provides a viable alternative – or pre-cursor supplement – to traditional geological and geomorphological mapping on regional to global scales where morphometrics are not the priority.

2. An overview of the grid-based mapping approach

Rather than delineating discrete geological or geomorphological units and features using points, lines, and polygons on a continuous mapping base, (i.e., “traditional” mapping approach), our grid-based mapping approach uses a simple identifier for the presence of a specific landform in each cell of an overlain grid. This work demonstrates the first example of grid mapping used on Mars, although earlier similar methods have been used for the Earth in few cases, for example, mapping of glacial bedforms and erosional zones in NW Scotland ([Bradwell, 2013](#)) and various statistical analyses in hydrometeorology ([Greene and Hudlow, 1982](#)). The first (reconnaissance) stage of the approach is to conduct context/reconnaissance mapping using regional or global scale datasets. For Mars, this could be a combination of MOLA terrain and, for example, THEMIS daytime IR image mosaics. In addition, the formal basemap for the study area must also be constructed. Importantly, the basemap data type must be of sufficient resolution to identify all the required landforms reliably, and must have continuous (or near continuous) image coverage. For the Martian northern plains study, we used CTX mosaics that had nearly complete coverage for each study area and that, with 6 m/px resolution, allowed decametre-scale landforms and surface textures to be identified. The aim of the context mapping is to: (i) identify large-scale features such as impact craters or large scale relief that provide topographic context, and (ii) to identify which specific landforms and terrain types will be systematically catalogued during the grid-based mapping. This suite of landforms can be either generic and include all the landforms seen within the area, or targeted in the context of a thematic geomorphological mapping programme. Either way, an important part of the reconnaissance stage is to study the basemap in detail and to produce a full inventory of the landform types that will be catalogued. If previous studies have identified the diversity of landforms that are present, the reconnaissance should be used to select, group, and sub-divide the landforms into a workable list of features. One advantage of the grid-based mapping approach is that it enables the efficient identification of multiple landform types through a single, systematic pass through the overlain grid; repeated passes to augment or refine landform types effectively undercuts this efficiency. Thus, we emphasize that the reconnaissance step is critical to the grid-based mapping approach.

In the second (mapping) stage, the mapping area is divided into a grid, which should offer a labelling and divisional system for ease of identification of data and for communication between mappers. This is best performed in a GIS setting using a shapefile or feature class. The

shapefile is given an attribute table, with a separate attribute for each landforms type to be studied and a unique identification code for each grid-square. The basemap imaging data are then systematically examined, grid-square by grid-square at full resolution (between 1:10,000 and 1:20,000 depending on the landforms present), in order to identify the landforms. Then, to record the spatial distribution of each of these landforms, their presence (or absence) in each grid-square is recorded in the grid-square shapefile attribute table. In our northern plains study, landforms were recorded as being either “present”, “absent” or “dominant.” The “dominant” classification was used when a single landform type covered the entire grid-square to such an extent that other landforms could have been obscured. Where relevant, each grid-square can also be recorded as “null” (meaning “no data”) or “possible” if there is uncertainty in identification, either when the mapper is unsure or when the image quality is poor but there is some evidence to suggest that the landform is present.

The result is a series of grids recording the distribution of all thematically relevant mapped landforms across the study area. In some ways, these are equivalent to raster images, as they show a continuous distribution-field of the various different landform types across a defined (rectangular, in most cases) area. When overlain on context maps, these form a coarse, digital landform distribution map.

In [Section 3.5](#) we describe in detail how we applied the approach to one area in Arcadia Planitia during the Mars’ northern plains mapping project. This provides both contextual discussion about the effectiveness of the approach and in-depth methods for the results stemming from this project.

3. Mapping the northern plains of Mars – the Arcadia Planitia study area

The northern plains project required mapping the spatial distribution of many ice-related landforms and surface types, in order to compare and contrast their distribution and generate hypotheses concerning their genesis. The northern plains comprise three main basin floors: Acidalia Planitia, Arcadia Planitia, and Utopia Planitia. A study area, consisting of a long latitudinal swath, was defined in each of these basins, with the precise location of the strips being selected largely based on the availability of high resolution images.

3.1. Cartographic projection

The study area in Arcadia is a 300 km wide strip extending from 30° to 80°N latitude, centred on the 170° West line of longitude. We opted to use a Cassini projection centred on the 170° West meridian. The Cassini projection is the transverse aspect of the commonly-used plate carrée, or equirectangular projection, with the equator at true scale. Where the plate carrée projection is based on a cylinder wrapped around the globe and tangent to the equator, the Cassini projection is a cylinder wrapped around the globe tangent to a chosen meridian. The advantage of this projection is that regions along the central meridian, and at right angles to it, have minimal distortion, making this projection ideal for long narrow north-south strips, like that of the three northern plains areas in this study.

3.2. Data and methods

Geomorphological analysis and mapping were performed primarily using publically available CTX images. CTX images were downloaded pre-processed, directly from the Arizona State University Mars Portal and ingested into a GIS (ESRI’s, Environmental Systems Research Institute, Inc. Redlands, CA, ArcGIS 10.1). MOLA gridded data and hill-shade products with around 1 m vertical accuracy, MOLA track data with around 150 m surface spot size point data and around 300 m along-track spacing ([Smith et al., 1993](#)), and THEMIS images were downloaded from the Planetary Data Systems’ Geosciences Node, Mars

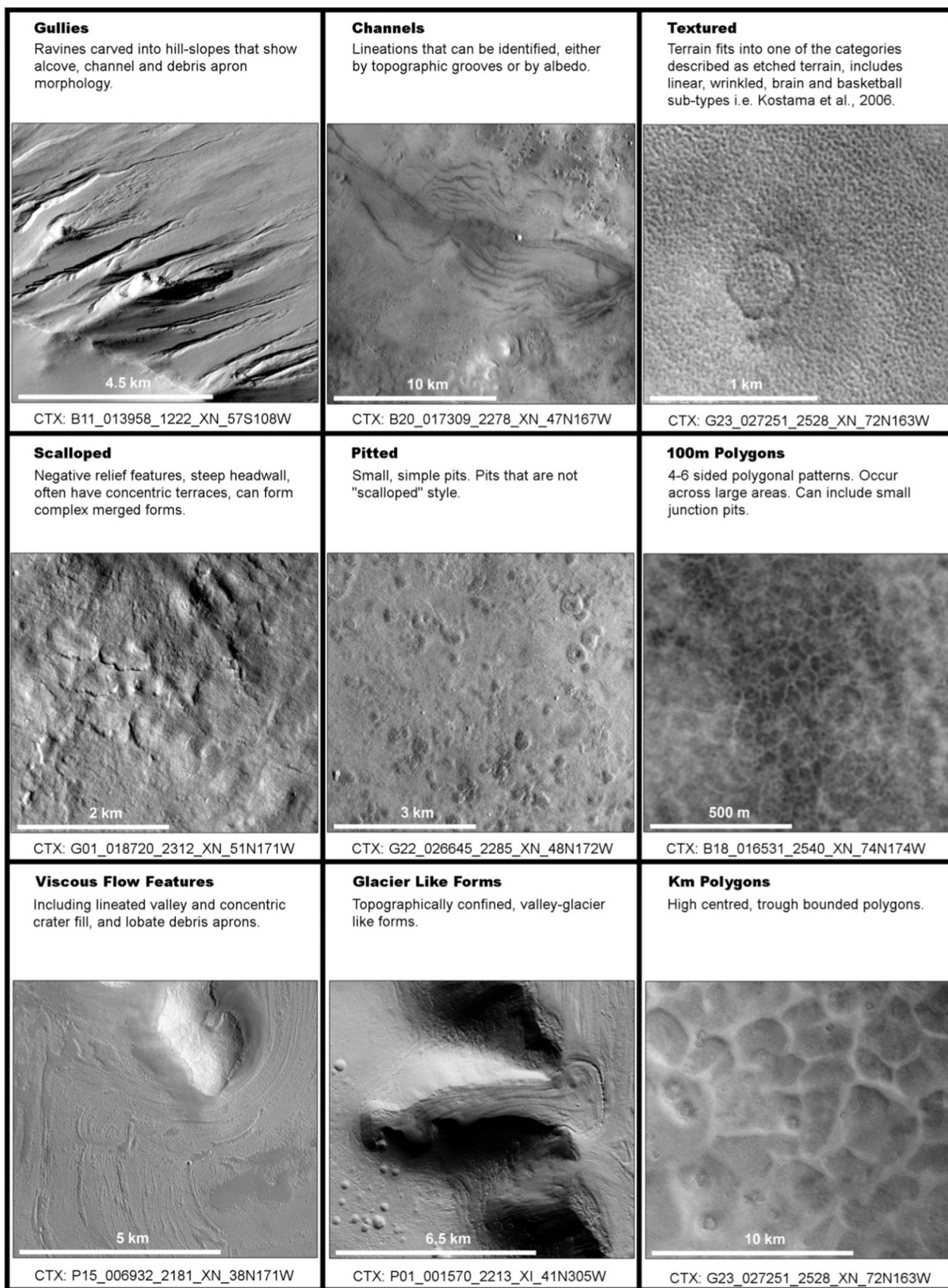


Fig. 1. Images showing examples of landforms selected of the ISSI mapping project. North is up and illumination from the south-west in all images. The last part of each CTX label gives the latitude and longitude.

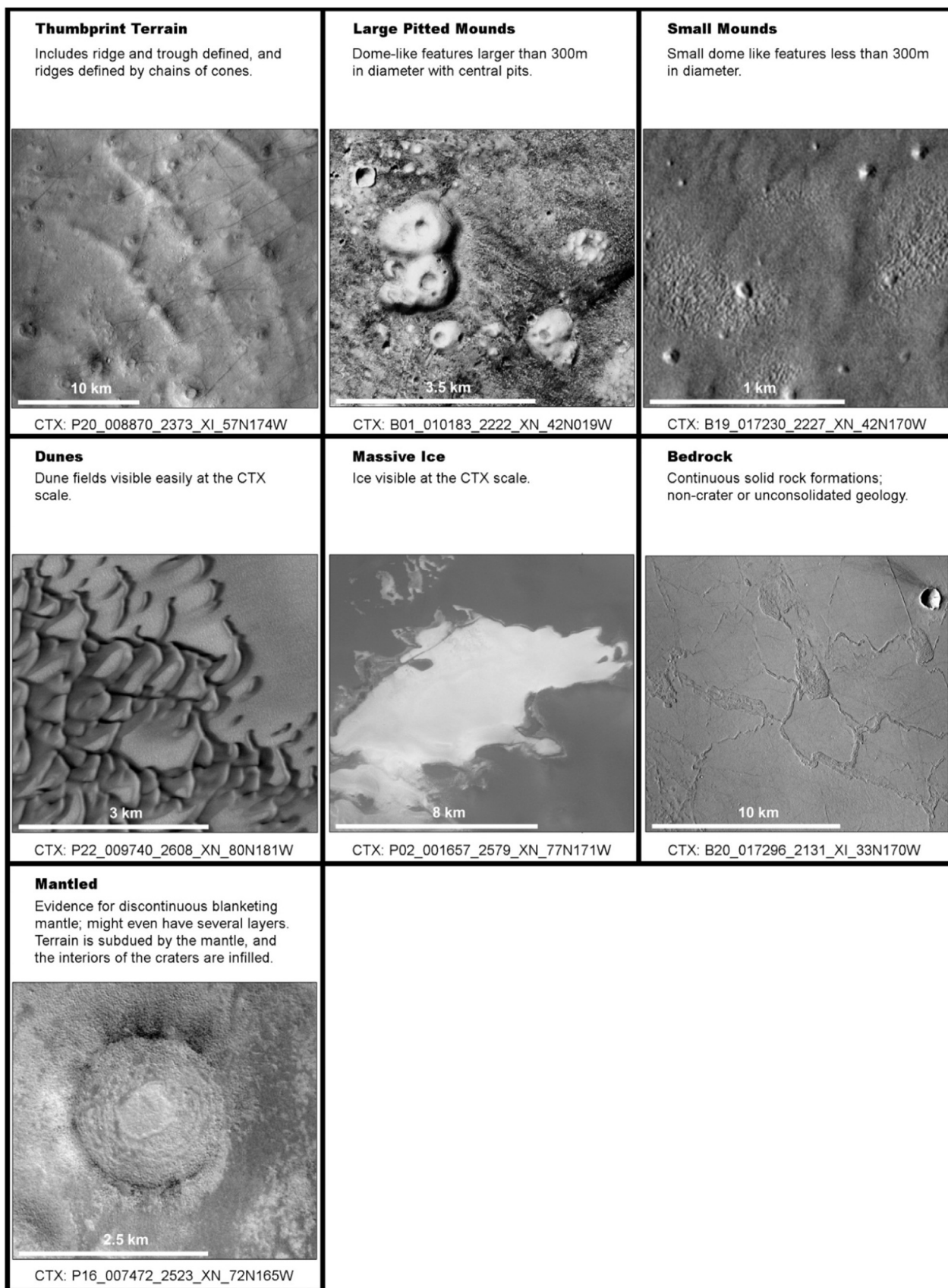


Fig. 1. (continued)

Orbital Data Explorer (ODE) and also ingested into the GIS.

The ESRI ArcGIS software package was used to display and manipulate the available datasets. Symbols were adapted from standard map drafting conventions (Federal Geographic Data Committee, 2006) and were provided as a package from the U.S. Geological Survey.

A simple reconnaissance map was created to give context to major relief and geological units. It used some of the line work from the published geological map of the northern plains of Mars (Tanaka et al., 2005), with additional features based on our reconnaissance. The map scale of our context mapping was at 1:10,000,000 (i.e., the Arcadia strip would be about 3 cm wide by 30 cm tall if printed at this scale). The digital scale is around 1:2,000,000 with approximately 2 km vertex spacing for digitised lines and polygons; these scales are incapable of conveying the occurrence of local decametre scale landforms individually. To identify the variety of landforms in the area, CTX images and THEMIS IR daytime images were overlaid onto MOLA hill-shade and elevation products. The suite of landforms identified within the Arcadia strip can be seen in Fig. 1 and the motivation for mapping these landforms in Table 1.

The mapping strip was divided into a 15 × 150 grid of squares, each 20 by 20 km. In ArcGIS, a polygon feature-class shapefile was produced, in which each grid-square was represented by a single square polygon object. In the attribute table of this shapefile, a new attribute for each landform type was added. The THEMIS IR day and CTX images were then viewed systematically at up to 1:10,000 scale for each grid-square and the presence or absence of each of the suite of landforms was recorded.

3.3. Landform selection

The choice of landforms to include within a suite for thematic grid-based mapping is highly project-dependant; when deciding which landforms to include, scale, thematic relevance and grouping of related landforms must be considered. For the northern plains project we chose landforms that have been cited as providing evidence of past or present ground ice (see Fig. 1), including viscous flow features (VFFs; Milliken et al., 2003), glacier like forms (GLFs; Hubbard et al., 2011; while we use the classification scheme reviewed by Souness and Hubbard, 2012,

we chose to map GLFs separately as they can often be identified as a distinct landform comparable with terrestrial analogues), ~100 m polygons (Mangold, 2005), scalloped and non-scalloped pits (which might have a thermokarstic origin; Costard and Kargel, 1995), and linear, wrinkled, brain and “basketball” terrain textures associated with the LDM (Kostama et al., 2006), which we have grouped under the class “Textured” for this study. In addition to searching for the textural signatures of the LDM, we also recorded instances of topographic infilling and relief softening that provided a topographic (rather than textural) indication of a draping mantle (likely the LDM; Kostama et al., 2006). We also chose to include landforms potentially indicative of thaw, such as gullies (e.g., Mellon and Phillips, 2001) and channels (e.g., Sharp and Malin, 1975).

Owing to their potential links with water/ice processes, the locations of kilometre-scale polygons, thumbprint terrain, large pitted mounds, and small mounds were recorded. The formation mechanism of the thumbprint terrain and associated large pitted mounds or cones is enigmatic and has been interpreted to be debris left behind after the removal of a static ice sheet (Grizzaffi and Schultz, 1989), rogen moraine – underwater glacial push moraine (Lockwood et al., 1992), mud volcanism (Davis and Tanaka, 1995), and various volcanic and lava/ice interaction features (Bridges et al., 2003; Bruno et al., 2004; Ghent et al., 2012; Plescia, 1980). Kilometre scale polygons or “giant polygons” are thought to be a product of tectonic, volcanic, dessication or compaction processes and could be a result of faulting and rebounding following the removal of a water/ice load (e.g. El Maarry et al., 2010; McGill and Hills, 1992; Pechmann, 1980). These kilometre-scale forms were mapped using a combination of THEMIS and CTX, as they could often be more easily seen in THEMIS than when ‘zoomed-in’ using CTX. Reconnaissance mapping revealed the presence of small mounds, typically small, featureless hills less than 30 m in diameter that are morphologically similar to rootless cones (e.g. Lanagan et al., 2001), pingos (Burr et al., 2009), or erosional remnants. Finally, we chose to include landforms that might obscure or explain the absence of other landforms, obscuring landforms include dune fields, massive ice (largely water ice that is “massive” in the spatial sense, not referring to geological layering) and continuous “bedrock” formations. An example of bedrock is the platy-ridged material inferred to be lava flows in

Table 1
showing the motivations for mapping the selected landforms with the scale of observations needed.

Landform	Approximate Observation Scale	Motivation	References
Mantled	Visible in CTX 1:20k	Evidence for ground ice, mantling deposit.	Kostama et al. (2006)
Textured	Visible in CTX 1:20k	Evidence for degradation of ground ice.	Kostama et al. (2006)
Pitted	Visible in CTX 1:20k	Evidence for degradation of ground ice.	Costard and Kargel (1995)
Scalloped Pits	Visible in CTX 1:20k	Evidence for degradation of ground ice.	Costard and Kargel (1995)
100 m Polygons	Visible in CTX 1:20k	Evidence for possible ground ice processes.	Mangold (2005)
Km Polygons	Visible in CTX/THEMIS 1:100k	Unknown origin, possible evidence for ground ice/water expulsion processes.	El Maarry et al. (2010); McGill and Hills (1992); Pechmann (1980)
Viscous-flow Features	Visible in CTX/THEMIS 1:200k	Evidence for flow of ice-rich material.	Milliken et al. (2003)
Glacier-like Forms	Visible in CTX 1:20k	Evidence for deposition, flow and reworking of ice-rich material against topographic obstacles.	Hubbard et al. (2011)
Thumbprint Terrain	Visible in CTX/THEMIS 1:200k	Unknown origin, possible evidence for glacial flow.	Grizzaffi and Schultz (1989); Lockwood et al. (1992); Davis and Tanaka (1995); Bridges et al. (2003); Bruno et al. (2004); Ghent et al. (2012); Plescia (1980)
Large Pitted Mounds	Visible in CTX 1:100k	Unknown origin, possible evidence for mud volcanism.	
Small Mounds	Visible in CTX 1:20k	Unknown origin, possible mud volcanism/ground ice processes/erosional remnants.	Lanagan et al. (2001); (Burr et al., 2009)
Channels	Variable CTX 1:20–200k	Evidence for liquid water, thaw.	Sharp and Malin (1975)
Gullies	Visible in CTX 1:20k	Evidence for liquid water, thaw.	Malin and Edgett (2000); Mellon and Phillips (2001)
Massive Ice	Visible in CTX/THEMIS 1:200k	Ice visible at the surface. Obscures possible evidence for ground ice.	Tanaka et al. (2005)
Dunes	Visible in CTX/THEMIS 1:200k	Evidence for wind-blown sand, Obscures possible evidence for ground ice.	Hayward et al. (2007) Tanaka et al. (2005)
Bedrock	Visible in CTX/THEMIS 1:200k	Evidence for solid rock, or no evidence for ground ice processes/landforms.	Tanaka et al. (2005)

Southern Arcadia/North Amazonis Planitia (Keszthelyi et al., 2000).

3.4. Verification of landform selection and the grid-based mapping approach: test mapping

To determine whether the grid-based mapping approach was viable for multiple mappers, and that the landforms we had selected were consistently identifiable, six mappers with varying levels of experience, both with the martian datasets and ArcGIS, were selected to apply the method to a test sample. The test sample had nine different areas, each with four 20 km by 20 km grid-squares. As per the grid-mapping protocol, each mapper analysed the CTX and THEMIS sample data to estimate the relative frequency of occurrence of each member of a predefined set of landforms by recording if each landform type was “present”, “dominant”, “absent” or “possible”, or if the availability of usable data was “null”. The six mappers each completed the attribute table in the shapefiles of their grid-based mapping results for these areas, hence allowing an estimate of how consistent the approach could be when applied to a larger scale project.

For each landform type in each square, we assigned a consistency rating based on the number of mappers agreeing on the relative frequency class describing each landform type in a given area. To calculate the consistency value, we recorded each mapper’s classification for each landform type. We interpreted the categories “present” and “dominating” as both meaning that a landform type is present. With 6 mappers, there were 28 possible outcomes, which can be seen in Fig. 2. The consistency ratings ranged from Consistent through Semi-Consistent to Inconsistent. For the evaluation of consistency, we counted entries of “possible” to be split between present and absent and hence that they were half in agreement with both “present” and “absent”. To be considered “consistent” at least five out of six mappers needed to agree on either the presence or absence of a landform. To be “inconsistent” less than four mappers had to agree on the presence or absence of a landform. Finally to be “semi-consistent” between four and five mappers had to agree on the presence or absence of a landform. Note that if five or six mappers were to assign a “possible” for a landform this would be evaluated as inconsistent in this evaluation. While it could be argued that the mappers were consistent in that they


Present or Dominating	Possible	Absent	
6	0	0	
5	1	0	
5	0	1	
4	2	0	
4	1	1	
4	0	2	
3	3	0	
3	2	1	
3	1	2	
3	0	3	
2	4	0	
2	3	1	
2	2	2	
2	1	3	
2	0	4	
1	5	0	
1	4	1	
1	3	2	
1	2	3	
1	1	4	
1	0	5	
0	6	0	
0	5	1	
0	4	2	
0	3	3	
0	2	4	
0	1	5	
0	0	6	

Fig. 2. A look-up table to show the 28 possible combinations of mappers’ responses for the test mapping with our consistency rating. “Present” and “dominating” are both have been grouped, we counted entries of “possible” to be split between present and absent. We deemed “consistent” as five out of six mappers agreeing, “inconsistent” as less than four mappers agreeing and “semi-consistent” as between four and five mappers agreeing.

agreed on the difficulty to say whether a specific landform was present or not, we took a more conservative approach, because no decision was made.

The results of the test mapping are shown in Fig. 3. Note that the suite of landform types in this test mapping was somewhat different from the final suite described above but the refinements to the final suite were made as a result of the test mapping. Our tests showed the rank classification of spatial frequency to be 70% consistent, 20% semi-consistent and 10% inconsistent. However, Fig. 3 highlights that some landform and terrain types are more difficult to identify than others. For example, the difficulties in distinguishing between brain terrain and basketball terrain in the tests resulted in us finally grouping the two types together with etched and linear terrains into a more inclusive “textured” terrain type. We found that loosely defined attributes such as “rough” and “smooth” were inconsistent and these labels were dropped following the test mapping.

3.5. Grid-mapping results

The results from the grid-based mapping are stored as attributes in a GIS shapefile. This data can be manipulated within a GIS to output a variety of products. The most basic of these products is shown in Fig. 4c, where the different shades represent the presence or absence of a single landform type in each grid-square. Dual landform type maps can be constructed by manipulating the data so that the grid-squares are coloured to show where two landforms overlap, occur singularly or not at all, as shown in Fig. 4d. Compilation landform type maps can be created by overlaying symbologies, as shown in Fig. 4b, to show multiple landforms types and compare their distributions within and between grid-squares. As the data are gridded, summary statistics can quickly be generated, tabulated, and manipulated using statistical software such as *R*. Consistently-sized grids also allow for rapid inter-area comparisons, both within and between entire mapping strips.

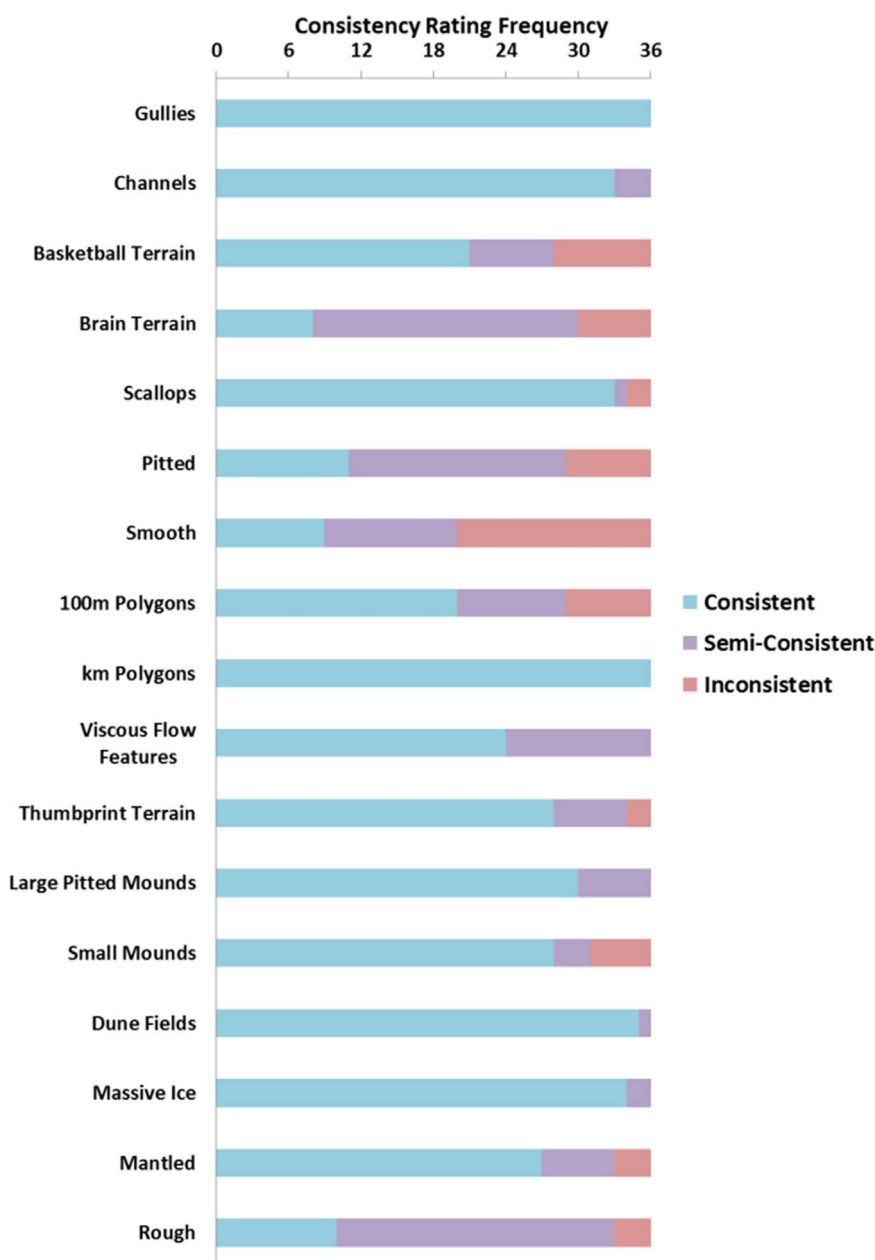


Fig. 3. Stacked-bar chart showing the consistency rating frequency for each landform or terrain type. $9 \times 4 (=36)$ individual grid squares were mapped.

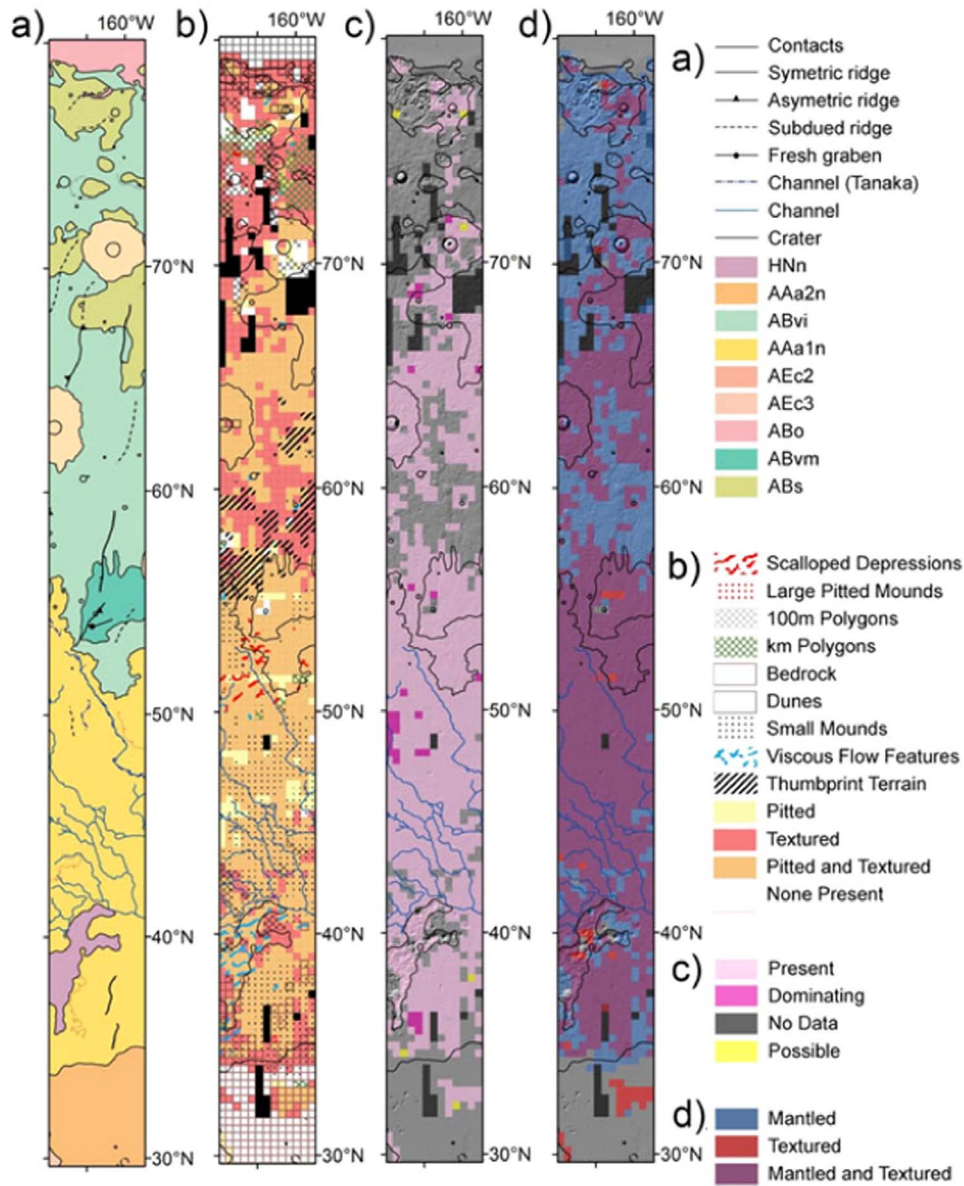


Fig. 4. Results from grid-mapping in Arcadia Planitia. a) An adaptation of the Geological Map of the northern plains of Mars (Tanaka et al., 2005) used as our reconnaissance map. b) Geomorphic Map using a compilation of grid-based mapping data. c) Grid-based mapping data showing the location of pits only. d) A dual landform map comparing and contrasting the presence of mantled and textured geomorphic signatures. b, c, and d, are all overlain onto a MOLA hillshade and outline extracts from the geological map in a.

3.6. Comparison with other data

The gridded data show where certain landform types occur, without consideration of age or landform density. While landforms do not determine geology, it may be that the landforms are controlled by geology. This makes landform occurrence data useful in delineating between surface units, determining contacts, and deriving geological maps in areas where the underlying geology is not immediately apparent. Equally, they can be used to generate statistical datasets for determining spatial associations between landform types and contextual attributes, such as topography, latitude, albedo or mineral/elemental abundances. Comparing the grid-based mapping results with other spatial datasets allows the identification of possible localised controls influencing the occurrence of specific landform types. For example, certain landforms are predisposed to occur only in certain topographic contexts; gullies require a slope to form, whereas polygons occur in flatter terrain within morphological units. As each entry in the dataset refers to a specific mapping grid-square, with a predefined size, other metrics such as terrain elevation mean, minimum, maximum and

range, slope type (concave, convex, rectilinear) and steepness, surface roughness and compositional properties (e.g. hydrogen and phyllosilicate abundance) can be added to the table, allowing for multivariate analysis of the effect of a range of local surface properties on the presence of each landform type.

4. Discussion

4.1. Advantages and disadvantages of grid-based mapping

There is a wide variety of both academic and applied studies that requires the acquisition, handling and analysis of large spatial datasets. While final map products are largely standardised, reconnaissance mapping is largely performed ad hoc. Standardising and converting reconnaissance data into a standardized map requires tremendous time and effort, meaning that the majority of data collected are not included in a formalised map. Grid-based mapping allows for efficient collection of large datasets that can be output in a consistent and easily comprehensible manner, complete with nominal to ordinal scale

statistics. Moreover, an efficient, consistent and standardised approach to spatial data collection makes it easier to share data and collaborate with partners and end users.

While the grid-based mapping approach is not a replacement for traditional mapping, it does provide an effective means of cataloguing multiple geomorphological landforms over large areas. This is due to the way interpretations are made through discrete decisions for small areas but mapping the extent of each landform type over large areas without having to physically locate and digitise boundaries or individual landforms. The technique becomes particularly advantageous when looking at vast and continuous high-resolution datasets, where there is a disparity between the scale of the final mapping output and the scale of data required to identify the landforms. Examples of high-resolution planetary datasets that can be used for landform identification include the terrestrial Landsat images, the Martian CTX and HRSC (High Resolution Stereo Camera; [Neukum and Jaumann, 2004](#)) images, and potentially images from the SIMBIO-SYS (Spectrometers and Imagers for MPO BepiColombo Integrated Observatory System; predicted global coverage at 50 m/pixel; [Flamini et al., 2010](#)) instruments on the yet to be launched BepiColombo mission to Mercury. For the northern plains of Mars mapping project, we catalogued potentially cryospheric landforms. However, this technique could be applied to a wider range of thematic data collection, targeting other genetic landform assemblages. The approach is particularly useful as first-pass reconnaissance as it provides both location and complementary contextual data and statistics to inform a more detailed study.

The main advantage of grid-based mapping is efficiency. For each area, a mapper has only to scan the image for the landforms in each of a range of landform types and record whether or not they are visible, removing the individual's decision about where to draw boundaries and what to include. This makes the process easier to implement for non-specialists. On average, we found it took around 2–3 min to complete the attribute table for each individual grid-square (20 km × 20 km). At the suggested grid sizes, it would take around an hour to complete 25 grid-squares (100 km × 100 km). If further resolution was needed, finer grids could be added. These would be able to carry the null and zero values forward from the coarser grids, meaning only areas with positive values for that landform would need to be examined, so that to increase the resolution for the whole strip, the whole map would not need to be re-examined. Therefore, it is a scalable approach. Similarly, if a landform type needs to be split into two or more different sub-categories, then only those grid-squares that contain the parent category need to be re-examined. Hence, a hierarchy of high spatial resolution and detailed classifications could be built up by employing smaller and smaller grids, and sub-classifying individual landform types, where needed.

Unlike traditional landform mapping, grid-based mapping enables a set of landforms, of multiple scales, to be catalogued efficiently in a single pass, minimising the time spent looking over the same images. However, if an additional landform type needed to be added later, it would require re-examining the whole dataset, meaning that starting with more landforms and combining classes afterwards if needed, is preferential. This also reinforces the need for good reconnaissance work, aimed at determining the total range of thematically relevant landform types in a study area.

As each grid-square is systematically searched, for each individual landform type, grid-based mapping rapidly ensures the whole mapping area is covered at full resolution, actively marking negative results. Thus, it is possible to distinguish between absence of landforms and absence of data. Both the mapping squares and the data collected by grid-based mapping are discrete meaning that grid-based mapping is scalable with group efforts. Transitions between colleagues are simpler to merge than using traditional mapping methods, as there are no contact lines or units to match up. However, to provide a consistent result, all mappers need to be able to come to a consensus on which individual landforms are going to be recorded under which landform

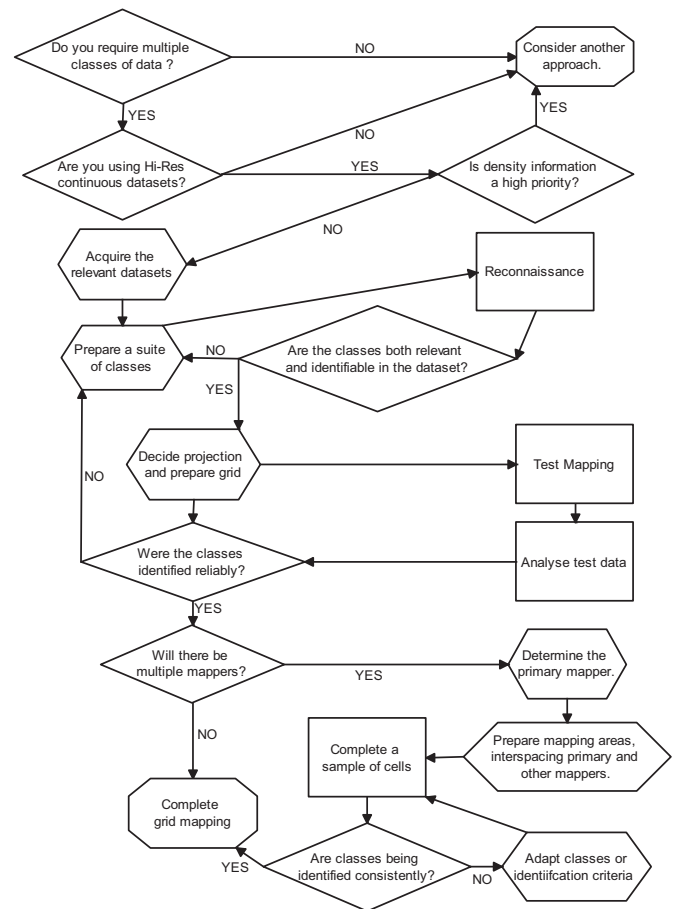


Fig. 5. Flow chart demonstrating an idealised work process for grid-based mapping. Diamonds represent decisions to be made by the mappers, hexagons for preparation steps, quadrangles for mapping stages and octagons for endpoints.

type. This is where reconnaissance and test mapping comparisons between mappers are advantageous. Note that this sort of checking system can be added to the approach to maximise inter-operator consistency by requiring certain grid-squares throughout the overall study area to be mapped by all mappers. With the grid-based mapping method there is the potential problem of double accounting of large discrete landforms. If large landforms occur on overlapping cells, they would likely be recorded twice. This is not a major issue for most situations but it is important to consider that some large landforms could be over represented by double counting.

The discrete data outputs for each landform type make it easy for comparisons between multiple landform types. This is particularly highlighted by the dual landform maps such as [Fig. 5d](#). The dual maps make it relatively easy to see where landforms appear to be mutually exclusive and where they consistently overlap, allowing landform assemblages to be constructed. The clearly defined grid also makes wider comparisons relatively easy, as multiple strips can be aligned alongside one another to check for spatial patterns and relationships, such as latitudinal trends.

The tabular nature of the dataset allows for effective statistical manipulation. Summary statistics can be produced through batch coding and quickly plotted to look for trends in large datasets. As each entry in the dataset refers to a specific area, with a predefined size, the resulting data are easily comparable with pre-existing datasets. To allow for direct comparison between the results of grid-based mapping and other data products it may be desirable to display other data in the grid-based mapping format. These can be used to compare results with, for example, mean, minimum, maximum and ranges of elevation, slope geometrics, surface roughness, surface concavity/convexity and com-

positional properties. This is particularly useful for assessing correlation between relief and landform types.

The main disadvantage of grid-based mapping is that it is an imprecise approach. The current method assigns the same weight to one landform as it does to a hundred. This could be easily modified, however, by entering a “percentage of the surface covered” estimate, or “number in the grid-square” when recording each landform type in the attribute table for each grid-square. On the other hand, this increases the time taken both to make decisions about the landforms and to enter the data, so a cost-benefit analysis must be made when modifying the approach. Another disadvantage to the grid mapping approach is that the method does not record morphometrics of landforms and only classifies landforms based on the categories determined while setting up the grid.

4.2. Selecting the landforms, cell size and approach

Grid-based mapping is most efficient when each grid is only viewed once, meaning that a project-specific “standardized” work plan, developed through reconnaissance, is essential. Key considerations when performing grid-based mapping are outlined in Fig. 5. The first considerations are whether multiple classes of data are required and whether high resolution, continuous datasets are available. If either is not, then a more traditional style of mapping or surveying may be more appropriate as the main benefit of grid-based mapping is being able to map the spatial distribution and relative spatial frequency of multiple landform types, and different sizes, over large spatial extents in one pass of the data. If the primary focus of the data collection is density information, grid-based mapping may not provide sufficient detail although it may be used initially to identify specific study areas. Once the approach has been decided upon, and the relevant datasets have been acquired, the suite of thematically relevant landform types needs to be predefined. To complete this vital stage, reconnaissance covering each mapping strip is required to confirm if the selected landform types are both relevant and consistently identifiable in the dataset(s). Subsequent to the definition of the thematically relevant suite of landform types, a projection that minimises distortion over the mapping strip must be chosen to allow for test mapping a sample of grid-squares. The purpose of the test mapping is to determine whether the landform types can be consistently identified over the entire mapping strip.

4.3. Cell completion order and possible shortcuts

When adopting a grid-based mapping approach, it is important to consider the order in which the cells will be completed. The most obvious approach might be to start systematically at one end of the grid and sequentially complete each cell before moving to the adjacent cell (See Fig. 6). A sequential approach has the advantage of it being immediately obvious how much of the project has been completed and how much is left to go. However, a sequential approach is very

inflexible and leaves the mapper no option but to complete the whole study area before even the most basic analysis can occur. A sequential approach can also lead to a cell completion order bias, if grids are completed systematically in one direction the mapper is more likely to carry decisions on whether a landform is present, or absent, forward, particularly for landforms that are difficult to identify. Where landforms extend over or cover more than one grid-square, a sequential approach could also lead to decisions on landform presence being cumulative, rather than being taken on a square by square basis. While this can dramatically speed up the completion of grids, it prevents the identification of mistaken or outlying cell entries, which removes an opportunity to check for self-consistency. Another option would be to complete grid-squares randomly, perhaps having them served through a random number generator. While this is an excellent way to minimise the problem of decisions made for one grid-square affecting the decisions made for surrounding grid-squares, it requires the mapper to complete the grid before being able to do any systematic analysis.

The mechanism we found to be most effective is to complete equally spaced grid-squares (such as every 2nd or every 3rd square) first, which can then be used to produce a coarse resolution landform map by extrapolating the results to surrounding grid-squares. This allows the mapper to review progress and assess the suitability of the grid dimensions and predefined thematically relevant attribute classes and, in addition, can be used to determine whether all grid-squares need to be populated to adequately represent the categorical range and distribution of landform types within the mapping strip. This equal spacing method also limits multi-cell decision making, as no completely adjacent grid-squares are analysed sequentially. This is likely to increase reliability but at the expense of time required to populate each grid-square.

It is important to note that increasing the size of a grid-square does not significantly decrease the time it takes to complete the grid-based mapping but does produce a coarser map. This is because the time taken to enter the data into the GIS is small compared to the time required to examine the data at full resolution and make decisions about the landforms. If full resolution is not required to classify the features, however, then use of larger grid-squares is appropriate and can speed up the task. However, there is a compromise to be made between the time spent completing attribute tables, time spent observing the images, and the resolution of the classified dataset.

4.4. Dividing the mapping

Considerations should be made when dividing the mapping between multiple mappers on how best to maintain consistency across the whole mapping strip (see Fig. 5). This can involve using overlapping areas to promote discussion and consolidation on how landforms are mapped. An alternative approach is to interweave regions to be mapped by secondary mappers with smaller areas to be mapped by a primary mapper, ensuring that all mapper boundaries are between the primary

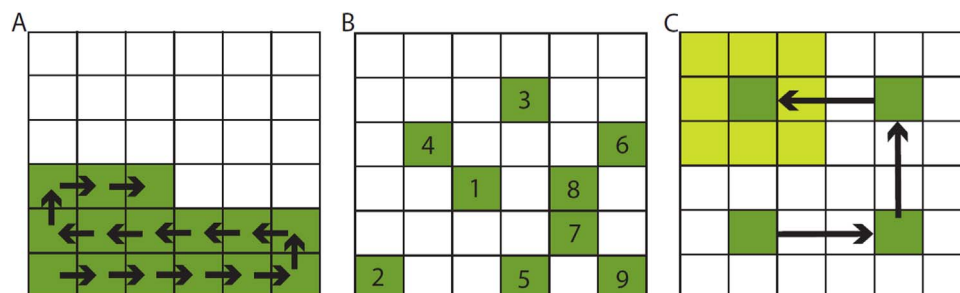


Fig. 6. A) Adjacent cell completion; cells are completed row by row sequentially. B) Randomised completion; each cell is assigned a random number and completed sequentially. C) Coarse resolution first completion; every third cell (dark green) is completed allowing results to extrapolated to adjacent cells (light green) to produce a coarse resolution raster. (For interpretation of the references to color in this figure legend, the reader is referred to the web version of this article.)

mapper and one secondary mapper. This allows for inter-operator consistency to be checked by one individual, helping to improve overall reliability.

4.5. Possible modifications to the approach

Grid-based mapping, as presented, provides little to no spatial density information on landform types. As the method is described, there is no mechanism to discriminate between a single instance of a landform type in a grid-square and many such landforms, perhaps covering a significant proportion of the grid-square. It is possible to produce a variation on how the data are recorded to include some density information; however this would come at the cost of both speed and ease of data collection. While not providing a definitive study on each individual landform type, which would require morphometrics of individual landforms in the type, this technique does provide an excellent way of cataloguing where landform types occur and could be used to target more focused and detailed research questions. It is worth noting that reclassifying the data to include spatial density information afterwards would not require looking through the entire dataset again, but only where landform types had been positively catalogued; and perhaps even then a sampled approach could be taken. One such approach could be to provide two attributes per landform type to be recorded for each grid-square, the first being confidence level on identification (i.e., present, probable or absent) the other a first order estimation of the number of landform of each type occurring in the grid-square. For point and linear landforms this could be recorded as an estimate of the population size of each landform type within each grid-square, for surface terrain types (*cf.* landcover classes) as estimated percentage coverage. This approach could provide an effective compromise between collecting density data and the time required to record each individual occurrence of a landform type.

4.6. Applications of the approach

The grid-based mapping approach has been developed to be applied to the Arcadia, Utopia and Acidalia regions of the martian northern plains. Other applications of the grid-based mapping method since include geomorphological mapping of Hellas (Voelker et al., 2015) and Lyot (Brooker et al., 2015) crater.

The discrete nature of the datasets also opens up the possibility for citizen science, crowdsourcing large mapping areas. Mapping areas can be divided and distributed to large numbers of participants. To improve reliability, individuals' results could be weighted against "experts" using control squares, experts being members of the appropriate science community who survey a sample of the mapping area. Searching for landforms in this manner would make possible the prospect of cataloguing landform types over the entire surface of Mars at CTX resolution. Crowdsourcing the task would be advantageous in that individuals could be selected as "specialists" in certain landforms, who could then perform more in-depth measurements on landform types that have been located by other users, providing an additional layer of information. Additional metrics such as the average time taken by the mapper to complete each grid-square could be recorded and provide an interesting and perhaps useful insight into the complexity of different regions.

With regard to a crowdsource grid-mapping effort, somewhat comparable studies are being performed by NASA's "Be a Martian" and "ClickWorkers" projects and Zooniverse's "Moon Zoo" project (Joy et al., 2011). These three projects utilized the advantageous numbers in citizen science largely to count and classify craters on planetary bodies. Although the data are largely yet to be published, preliminary observations and analysis (e.g. Kanefsky et al., 2001) are promising. The data collected by citizens in Kanefsky et al. (2001) was shown to be reliable against that collected by Nadine Barlow, an "expert" with several years of experience in crater counting. This encourages the consideration of applying a "grid-based mapping by citizen science"

approach to map landforms across the northern plains and, potentially, the entire surface of Mars.

5. Conclusions

A grid-based mapping approach provides an efficient solution to the problems of mapping small landforms over large areas by providing a consistent and standardised approach to spatial data collection. Moreover, it makes data sharing and collaboration easier, more consistent, flexible, and effective. Unlike with traditional landform mapping, grid-based mapping is able to catalogue a set of landform types, of multiple sizes, efficiently in a single pass, minimising the time spent looking over the same images. The discrete, tabular nature of the dataset allows for effectual statistical manipulation for assessing correlation between landform types, relief, relationships and trends. The simplicity of the approach makes grid-based mapping extremely scalable and workable for group efforts, requiring minimal user experience and producing consistent and repeatable results. The discrete nature of the datasets, simplicity of approach, and divisibility of tasks, open up the possibility of citizen science, in which crowdsourcing large grid-based mapping areas could be applied. A potential application of a "grid-based mapping by citizen science" approach would be to map landforms across the entire surface of Mars.

Acknowledgements

JR was supported by STFC (ST/L000776/1 and ST/K502212/1). MB was supported by grants from STFC (ST/L000776/1) and the UK Leverhulme Trust (RPG-397). SC was supported by the Leverhulme Trust (RPG-397) and the French Space Agency CNES. M.R.P. AL was supported by grant NCN (UMO-2013/08/S/ST10/00586). CO was supported by the ERASMUS program and BMWi grant 50QM1301.

References

- Balme, M., Berman, D.C., Bourke, M.C., Zimbleman, J.R., 2008. Transverse aeolian ridges (TARs) on Mars. *Geomorphology* 101, 703–720. <http://dx.doi.org/10.1016/j.geomorph.2008.03.011>.
- Barlow, N.G., Bradley, T.L., 1990. Martian impact craters: correlations of ejecta and interior morphologies with diameter, latitude, and terrain. *Icarus* 87, 156–179. [http://dx.doi.org/10.1016/0019-1035\(90\)90026-6](http://dx.doi.org/10.1016/0019-1035(90)90026-6).
- Batson, R.M., Bridges, P.M., Inge, J.L., 1979. Atlas of Mars. The 1:5,000,000 Map Series.
- Berman, D.C., Balme, M.R., Rafkin, S.C.R., Zimbleman, J.R., 2011. Transverse aeolian ridges (TARs) on Mars II: distributions, orientations, and ages. *Icarus* 213, 116–130. <http://dx.doi.org/10.1016/j.icarus.2011.02.014>.
- Bradwell, T., 2013. Identifying palaeo-ice-stream tributaries on hard beds: mapping glacial bedforms and erosion zones in NW Scotland. *Geomorphology* 201, 397–414. <http://dx.doi.org/10.1016/j.geomorph.2013.07.014>.
- Bridges, J.C., Seabrook, A.M., Rothery, D.A., Kim, J.R., Pillinger, C.T., Sims, M.R., Golombek, M.P., Duxbury, T., Head, J.W., Haldemann, A.F.C., Mitchell, K.L., Muller, J.-P., Lewis, S.R., Moncrieff, C., Wright, I.P., Grady, M.M., Morley, J.G., 2003. Selection of the landing site in Isidis Planitia of Mars probe Beagle 2. *J. Geophys. Res. Planets* 108, 5001. <http://dx.doi.org/10.1029/2001JE001820>.
- Brooker, L., Balme, M., Conway, Hagermann, A., Collins, G., 2015. Preliminary grid mapping of fluvial, glacial and periglacial landforms in and around Lyot crater. In: Proceedings of the Mars European Planetary Science Congress 2015 Held 27 Sept. to 2 Oct. 2015 Nantes Fr. Online [Http://meetingorganizer.copernicus.org/EPSC2015](http://meetingorganizer.copernicus.org/EPSC2015) IdEPSC2015-810 10, EPSC2015-810.
- Bruno, B.C., Fagents, S.A., Thordarson, T., Baloga, S.M., Pilger, E., 2004. Clustering within rootless cone groups on Iceland and Mars: effect of nonrandom processes. *J. Geophys. Res. E Planets* 109, 1–11. <http://dx.doi.org/10.1029/2004JE002273>.
- Burr, D.M., Tanaka, K.L., Yoshikawa, K., 2009. Pingos on Earth and Mars. *Planet. Space Sci.* 57, 541–555. <http://dx.doi.org/10.1016/j.pss.2008.11.003>.
- Christensen, P.R., Jakosky, B.M., Kieffer, H.H., Malin, M.C., Jr, H.Y.M., Neelson, K., Mehall, G.L., Silverman, S.H., Ferry, S., Caplinger, M., Ravine, M., 2004. The thermal emission imaging system (THEMIS) for the Mars2001 odyssey mission. *Space Sci. Rev.* 110, 85–130. <http://dx.doi.org/10.1023/B:SPAC.0000021008.16305.94>.
- Costard, F.M., Kargel, J.S., 1995. Outwash plains and thermokarst on Mars. *Icarus* 114, 93–112. <http://dx.doi.org/10.1006/icar.1995.1046>.
- Davis, P.A., Tanaka, K.L., 1995. Curvilinear ridges in Isidis Planitia, Mars—the result of mud volcanism. *Lunar Planet Sci. Conf.* 321–322.
- El Maarry, M.R., Markiewicz, W.J., Mellon, M.T., Goetz, W., Dohm, J.M., Pack, A., 2010. Crater floor polygons: desiccation patterns of ancient lakes on Mars? *J. Geophys. Res. Planets* 115, E10006. <http://dx.doi.org/10.1029/2010JE003609>.
- Federal Geographic Data Committee, 2006. FGDC Digital Cartographic Standard for

- Geologic Map Symbolization. Reston, Va., Federal Geographic Data Committee Document Number FGDC-STD-013-2006, 2.
- Flamini, E., Capaccioni, F., Colangeli, L., Cremonese, G., Doressoundiram, A., Jossel, J.L., Langevin, Y., Debei, S., Capria, M.T., De Sanctis, M.C., Marinangeli, L., Massironi, M., Mazzotta Epifani, E., Naletto, G., Palumbo, P., Eng, P., Roig, J.F., Caporali, A., Da Deppo, V., Erard, S., Federico, C., Forni, O., Sgavetti, M., Filacchione, G., Giacomini, L., Marra, G., Martellato, E., Zusi, M., Cosi, M., Bettanini, C., Calamai, L., Zaccariotto, M., Tommasi, L., Dami, M., Ficai Veltroni, J., Poulet, F., Hello, Y., 2010. SIMBIO-SYS: The spectrometer and imagers integrated observatory system for the BepiColombo planetary orbiter. *Planet. Space Sci., Comprehensive Science Investigations of Mercury: The Scientific Goals of the Joint ESA/JAXA Mission BepiColombo*, vol. 58, pp. 125–143. <http://doi.org/10.1016/j.pss.2009.06.017>.
- Ghent, R.R., Anderson, S.W., Pithawala, T.M., 2012. The formation of small cones in Isidis Planitia, Mars through mobilization of pyroclastic surge deposits. *Icarus* 217, 169–183. <http://dx.doi.org/10.1016/j.icarus.2011.10.018>.
- Greeley, R., Guest, J.E., 1987. Geologic map of the eastern equatorial region of Mars. *Greene, D.R., Hudlow, M.D., 1982. Hydrometeorologic grid mapping procedures*. In: *Proceedings of the AWRA International Symposium on Hydrometeorology*, Denver, CO.
- Grizzaffi, P., Schultz, P.H., 1989. Isidis basin: site of ancient volatile-rich debris layer. *Icarus* 77, 358–381. [http://dx.doi.org/10.1016/0019-1035\(89\)90094-8](http://dx.doi.org/10.1016/0019-1035(89)90094-8).
- Hayward, R.K., Mullins, K.F., Fenton, L.K., Hare, T.M., Titus, T.N., Bourke, M.C., Colaprete, A., Christensen, P.R., 2007. Mars Global Digital Dune Database and initial science results. *J. Geophys. Res. Planets* 112, E11007. <http://dx.doi.org/10.1029/2007JE002943>.
- Hubbard, B., Milliken, R.E., Kargel, J.S., Limaye, A., Souness, C., 2011. Geomorphological characterisation and interpretation of a mid-latitude glacier-like form: hellas Planitia, Mars. *Icarus* 211, 330–346. <http://dx.doi.org/10.1016/j.icarus.2010.10.021>.
- Jones, A.P., McEwen, A.S., Tornabene, L.L., Baker, V.R., Melosh, H.J., Berman, D.C., 2011. A geomorphic analysis of Hale crater, Mars: the effects of impact into ice-rich crust. *Icarus* 211, 259–272. <http://dx.doi.org/10.1016/j.icarus.2010.10.014>.
- Joy, K., Crawford, I., Grindrod, P., Lintott, C., Bamford, S., Smith, A., Cook, A., Zoo, M., 2011. Moon Zoo: citizen science in lunar exploration. *Astron. Geophys* 52, 2.10–2.12. <http://dx.doi.org/10.1111/j.1468-4004.2011.52210.x>.
- Kanefsky, B., Barlow, N.G., Gulick, V.C., 2001. Can distributed volunteers accomplish massive data analysis tasks? Presented at the Lunar and Planetary Science Conference.
- Kargel, J.S., Strom, R.G., 1992. Ancient glaciation on Mars. *Geology* 20, 3–7. [http://dx.doi.org/10.1130/0091-7613\(1992\)020<0003:AGOM>2.3.CO;2](http://dx.doi.org/10.1130/0091-7613(1992)020<0003:AGOM>2.3.CO;2).
- Kargel, J.S., Baker, V.R., Begét, J.E., Lockwood, J.F., Péwé, T.L., Shaw, J.S., Strom, R.G., 1995. Evidence of ancient continental glaciation in the Martian northern plains. *J. Geophys. Res. Planets* 100, 5351–5368. <http://dx.doi.org/10.1029/94JE02447>.
- Keszthelyi, L., McEwen, A.S., Thordarson, T., 2000. Terrestrial analogs and thermal models for Martian flood lavas. *J. Geophys. Res. Planets* 105, 15027–15049. <http://dx.doi.org/10.1029/1999JE001191>.
- Kostama, V.-P., Kreslavsky, M.A., Head, J.W., 2006. Recent high-latitude icy mantle in the northern plains of Mars: characteristics and ages of emplacement. *Geophys. Res. Lett.* 33, L11201. <http://dx.doi.org/10.1029/2006GL025946>.
- Kreslavsky, M.A., Head, J.W., 2002. Mars: nature and evolution of young latitude-dependent water-ice-rich mantle. *Geophys. Res. Lett.* 29. <http://dx.doi.org/10.1029/2002GL015392>.
- Lanagan, P.D., McEwen, A.S., Keszthelyi, L.P., Thordarson, T., 2001. Rootless cones on Mars indicating the presence of shallow equatorial ground ice in recent times. *Geophys. Res. Lett.* 28, 2365–2367. <http://dx.doi.org/10.1029/2001GL012932>.
- Lockwood, J.F., Kargel, J.S., Strom, R.B., 1992. Thumbprint terrain on the northern plains: a glacial hypothesis. Presented at the Lunar and Planetary Science Conference, p. 795.
- Lucchitta, B.K., Ferguson, H.M., Summers, C., 1986. Sedimentary deposits in the Northern Lowland Plains, Mars. *J. Geophys. Res. Solid Earth* 91, E166–E174. <http://dx.doi.org/10.1029/JB091iB13p0E166>.
- Malin, M.C., Edgett, K.S., 2000. Evidence for recent groundwater seepage and surface runoff on Mars. *Science* 288, 2330–2335. <http://dx.doi.org/10.1126/science.288.5475.2330>.
- Malin, M.C., Bell, J.F., Cantor, B.A., Caplinger, M.A., Calvin, W.M., Clancy, R.T., Edgett, K.S., Edwards, L., Haberle, R.M., James, P.B., Lee, S.W., Ravine, M.A., Thomas, P.C., Wolff, M.J., 2007. Context camera investigation on board the Mars reconnaissance orbiter. *J. Geophys. Res. Planets* 112. <http://dx.doi.org/10.1029/2006JE002808>.
- Mangold, N., 2005. High latitude patterned grounds on Mars: classification, distribution and climatic control. *Icarus* 174, 336–359. <http://dx.doi.org/10.1016/j.icarus.2004.07.030>.
- McGill, G.E., Hills, L.S., 1992. Origin of giant Martian polygons. *J. Geophys. Res. Planets* 97, 2633–2647. <http://dx.doi.org/10.1029/91JE02863>.
- Mellon, M.T., Phillips, R.J., 2001. Recent gullies on Mars and the source of liquid water. *J. Geophys. Res. Planets* 106, 23165–23179. <http://dx.doi.org/10.1029/2000JE001424>.
- Milliken, R.E., Mustard, J.F., Goldsby, D.L., 2003. Viscous flow features on the surface of Mars: Observations from high-resolution Mars Orbiter Camera (MOC) images. *J. Geophys. Res. Planets* 108. <http://dx.doi.org/10.1029/2002JE002005>.
- Neukum, G., Jaumann, R., 2004. HRSC: the High Resolution Stereo Camera of Mars Express. In: *Mars Express: The Scientific Payload*. Presented at the Mars Express: the Scientific Payload, pp. 17–35.
- Otto, J.C., Smith, M.J., 2013. Geomorphological Mapping. *Geomorphological Techniques* (online edition). British Society for Geomorphology, London (2047-0371).
- Pechmann, J.C., 1980. The origin of polygonal troughs on the northern Plains of Mars. *Icarus* 42, 185–210. [http://dx.doi.org/10.1016/0019-1035\(80\)90071-8](http://dx.doi.org/10.1016/0019-1035(80)90071-8).
- Peulvast, J.-P., Mège, D., Chiciak, J., Costard, F., Masson, P.L., 2001. Morphology, evolution and tectonics of Valles Marineris wallslopes (Mars). *Geomorphology* 37, 329–352. [http://dx.doi.org/10.1016/S0169-555X\(00\)00085-4](http://dx.doi.org/10.1016/S0169-555X(00)00085-4).
- Plescia, J.B., 1980. Cinder cones of Isidis and Elysium. *Rep. Planet. Geol. Program* 1, 263–265.
- Robbins, S.J., Hynek, B.M., 2012. A new global database of Mars impact craters ≥ 1 km: 1. Database creation, properties, and parameters. *J. Geophys. Res. Planets* 117, E05004. <http://dx.doi.org/10.1029/2011JE003966>.
- Scott, D.H., Carr, M.H., 1978. Geologic Map of Mars.
- Scott, D.H., Tanaka, K.L., 1986. Geologic Map of the Western Equatorial Region of Mars.
- Sharp, R.P., Malin, M.C., 1975. Channels on Mars. *Geol. Soc. Am. Bull.* 86, 593–609. [http://dx.doi.org/10.1130/0016-7606\(1975\)86<593:COM>2.0.CO;2](http://dx.doi.org/10.1130/0016-7606(1975)86<593:COM>2.0.CO;2).
- Skinner Jr., J.A., Hare, T.M., Tanaka, K.L., 2006. Digital renovation of the Atlas of Mars 1:15,000,000-scale global Geologic Series maps. In: *Proceedings of the Lunar Planetary Science Conference* 37, #2331. (abstract)(online).
- Smith, D.E., Zuber, M.T., Abshire, J.B., 1993. Mars Observer Laser Altimeter investigation. pp. 14–18. <http://doi.org/10.1117/12.157137>.
- Souness, C., Hubbard, B., 2012. Mid-latitude glaciation on Mars. *Prog. Phys. Geogr.* 36, 238–261. <http://dx.doi.org/10.1177/0309133312436570>.
- Souness, C., Hubbard, B., Milliken, R.E., Quincey, D., 2012. An inventory and population-scale analysis of martian glacier-like forms. *Icarus* 217, 243–255. <http://dx.doi.org/10.1016/j.icarus.2011.10.020>.
- Tanaka, K.L., Scott, D.H., 1987. Geologic Map of the Polar Regions of Mars.
- Tanaka, K.L., Isbell, N.K., Scott, D.H., Greeley, R., Guest, J.E., 1988. The resurfacing history of Mars: a synthesis of digitized, Viking-based geology. *Lunar Planet. Sci. Conf.* 18, 665–678.
- Tanaka, K.L., Skinner, J.A., Hare, T.M., 2005. Geologic Map of the Northern Plains of Mars.
- Tanaka, K.L., Skinner Jr., J.A., Dohm, J.M., Rossman, R.L.I., Kolb, E.J., Fortezzo, C.M., Platz, T., Michael, G.G., Hare, T.M., 2014. Geologic Map of Mars.
- Tanaka, K.L., Robbins, S.J., Fortezzo, C.M., Skinner Jr., J.A., Hare, T.M., 2014. The digital global geologic map of Mars: Chronostratigraphic ages, topographic and crater morphologic characteristics, and updated resurfacing history. *Planet. Space Sci., Planetary Geology Field Symposium, Kitakyushu, Japan, 2011: Planetary Geology and Terrestrial Analogs* 95, pp. 11–24. <http://doi.org/10.1016/j.pss.2013.03.006>.
- Ulrich, M., Wagner, D., Hauber, E., de Vera, J.-P., Schirmer, L., 2012. Habitable periglacial landscapes in martian mid-latitudes. *Icarus* 219, 345–357. <http://dx.doi.org/10.1016/j.icarus.2012.03.019>.
- Voelker, M., Hauber, E., van Gassel, S., Jaumann, R., 2015. Grid Mapping of Hellas Planitia – preliminary results from the northern impact rim. In: *Proceedings of the European Planetary Science Congress10*, Presented at the European and Planetary Science Congress, Nantes, Frankreich.
- Wilson, S.A., Zimbelman, J.R., 2004. Latitude-dependent nature and physical characteristics of transverse aeolian ridges on Mars. *J. Geophys. Res. Planets* 109, E10003. <http://dx.doi.org/10.1029/2004JE002247>.